

MODELLING OF PRELOADED REINFORCED-CONCRETE STRUCTURES AT DIFFERENT LOADING RATES

A. Bach^{1,4}, A. Stolz^{2,4}, M. Nöldgen³ and K.Thoma²

¹ Schüßler-Plan Ingenieurgesellschaft mbH, Düsseldorf, Germany

e-mail: abach@schuessler-plan.de

² Fraunhofer-Institute for High-Speed Dynamics, Ernst-Mach-Institut, Efringen-Kirchen, Germany

³ Cologne University of Applied Science, CUAS, Cologne, Germany

⁴ BRS-Design: www.brs-design.com

Keywords: Reinforced Concrete, Preload, SDOF, FEM, Plastic Hinge, Loading Rates

Abstract: For the modeling of reinforced concrete structures under quasi-static, dynamic and impulsive loading different approaches are commonly used within the analysis, such as the Single Degree Of Freedom (SDOF) approach, finite element methods using implicit or explicit methods and hydrocode simulations. The proposed paper sates the possibility for the description of the structural dynamic behavior of reinforced concrete using two different SDOF Method based on experimental shock tube tests on single-span reinforced concrete-slabs and analyses their applicability regarding plastic hinge formation. Furthermore studies on the effects of preloading for a representative structural element will be carried out, which allow for an indication of the influence of preload on the dynamic resistance of structural elements. This will help to analyse reinforced concrete from the quasi-static to the dynamic and impulsive domain of response at different loading rates under preloaded conditions.

1 INTRODUCTION

Modelling of reinforced concrete structures under accidental load cases, such as explosion, impact or fires, requires precise state of the art approaches to describe the structure under regular and accidental loading conditions.

Different approaches are applicable for the description of reinforced concrete under static and dynamic loading such as single degree of freedom (SDOF) or finite element methods (FEM).

These approaches may differ in their level of description and complexity but need to be able to describe the nonlinear behaviour of reinforced concrete structures accurately.

For an accurate description of dynamic problems these methods should be capable of describing the structural behaviour within the dynamic but also in the static domain as preload may influence the results. An indication of the impact of preload has been given by Riedel [1] and Krauthammer [2].

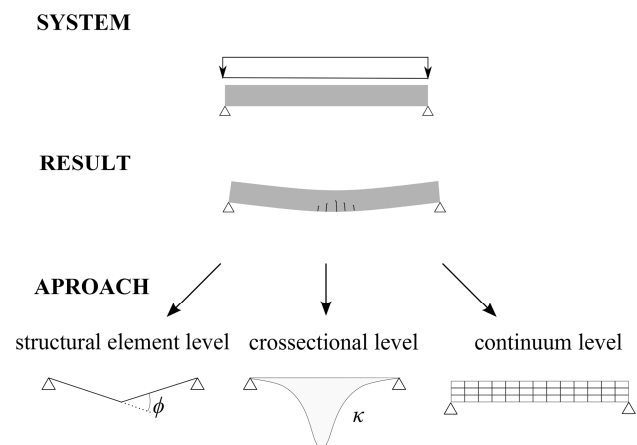


Figure 1: Approaches for the description non-linear description of reinforced concrete members.

The represented paper will describe the commonly used SDOF approaches on the cross-sectional and structural element level according to the UFC-3-340 [3] for the description of dynamic loads (chapter 2) and show their applicability on shock tube experiments on reinforced concrete plates

(chapter 3). Further on effects of transverse preload will be discussed in (chapter 4) and magnitudes presented for the impact of preload on the dynamic resistance using PI-curves. In addition to the SDOF-Method the application of hydrocode simulations for the description of the dynamic behaviour of reinforced concrete and effects of preload are shown. As the hydrocode method will be used in the future for deriving aspects of preload on high-speed dynamic loads and may therefore be used as general methodology for the description of preloaded reinforced concrete members under dynamic as well as high-speed dynamic loadings.

2 SDOF METHOD

The SDOF-Method is a widely used method for the analysis and design of members subjected to dynamic loads. The method may be used for the evaluation of the response of structures or structural members subjected to earthquakes [4, 5], explosions [6, 7] or impact [8].

Like for most dynamic problems the concept of the SDOF arises from the necessity of solving the equation of motion. The SDOF relates the answer of the structural member to one shape function $\phi(x)$, wherefore the displacement of the overall system $w(x,t)$ is described by one degree of freedom (1).

$$w(x,t) = \phi(x) \cdot u(t) \quad (1)$$

Therefore the equation of motion of the overall of the system can be described by one freedom u solely [3, 6, 7, 9].

$$\begin{aligned} k_{lm} \cdot M \cdot \ddot{u} + R(u) &= F(t) \\ M_E \cdot \ddot{u} + R(u) &= F(t) \end{aligned} \quad (2)$$

The effective mass M_E is calculated according to the variation principles [9, 10] to ensure equilibrium of internal, kinetic and potential energy of the system. The value of the load-mass factor k_{lm} depends on the assumed shape function. Values for different

static systems are given in [3].

With mass and load acting on the structure known the definition of the load deflection characteristic of the structural member is essential for the application of the SDOF method.

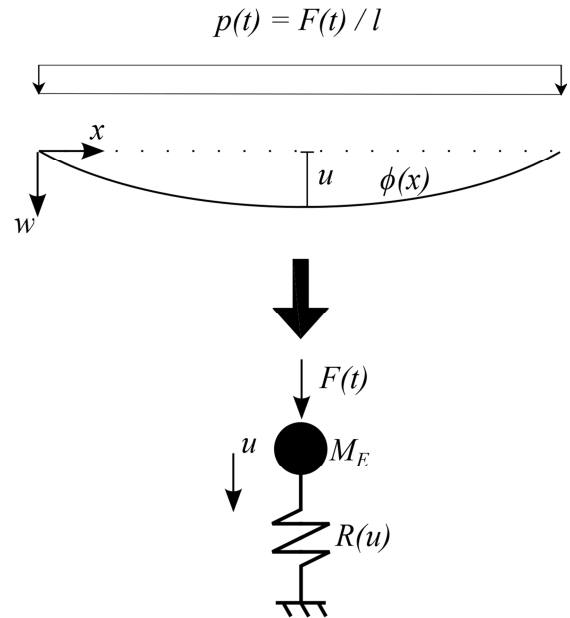


Figure 2: Transformation of Structural System to a SDOF.

For reinforced concrete section the load resistance curves needs to be calculated in a way, such that the non-linear structural behaviour of the reinforced concrete can be described accurately. This includes the elastic response (phase I), the development of cracks (phase II) and the development of plasticity due to the yielding of the reinforcement (phase III) up to failure due to rapture of the reinforcement or crushing of the concrete [11].

Two approaches are hereby feasible: The description on the structural element level based on theory of plasticity or on the cross-sectional level. Whereby the structural element approach is a simplification of the cross-sectional approach as shown in the following.

CROSS-SECTIONAL APPROACH

The cross-sectional approach is based on the moment-curvature-relationship using the thesis of Navier-Bernoulli, which states that for beams, thin plates and shells the strain distribution over the depth of beams remains linear and hence the curvature constant.

The validity of this thesis for the elastic and plastic behaviour of RC-Beams has been shown in many experiments i.e. by Dilger and Leonhard [11, 12].

Therefore for given axial and bending loads the strain distribution of the crosssection can be found iteratively satisfying equilibrium between the forces (N and M) and the stresses using uniaxial stress-strain relationships, see Eq. 3 and Figure 3.

$$\int_0^h \sigma(z) \cdot b \cdot dz = N$$

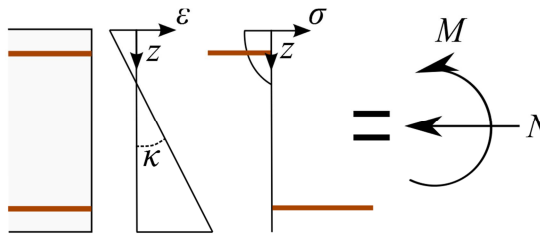
$$\int_0^h \sigma(z) \cdot z \cdot b \cdot dz = M \quad (3)$$


Figure 3: Stress-Strain Relationship for a Reinforced Concrete Section under bending.

Hereby the bound of concrete and reinforcement between the cracks, known as tension stiffening, should be taken into account as otherwise the maximum displacement will be overestimated leading to an overestimation of the strain energy. Approaches for considering tension stiffening are given in [13].

The average trilinear Moment-Curvature can be calculated according to the following steps:

1. Evaluation of the maximum elastic Moment (M_{cr}) and curvature (κ_{cr}) until cracking of the concrete occurs and

calculation of the average tension stiffening.

2. Evaluation of yield Moment (M_y) and curvature (κ_y) for steel strain equal to ε_{sy} and the related average yield curvature by iteration over the cross section satisfying Eq. 3.
3. Ultimate Moment (M_u) and (κ_u) curvature defined by crushing of the concrete (ε_{cu}) or rupture of the reinforcement (ε_{su}) and the related average ultimate curvature by iteration over the cross section satisfying Eq. 3.

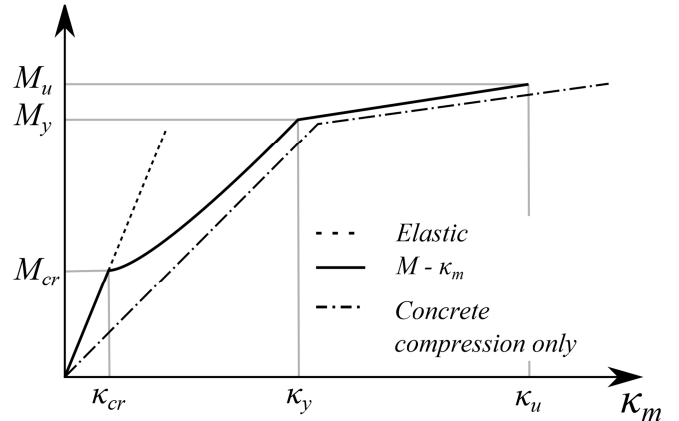


Figure 4: Schematic Moment-Curvature Relationship including tension stiffening.

From the moment curvature relationship the displacement for a given loading can be derived under respect to the given boundaries by double integration. Hence the displacement at mid-span for a singly supported beam can be derived from the curvature of the given moment distribution.

STRUCTURAL ELEMENT APPROACH

The structural element approach defines the resistance on the structural level and is based on plastic limit analysis. As the original plastic limit analysis assumes infinite rotation of the plastic hinges, no conclusions can be drawn for the displacement. For static problems the displacement is of minor interest as only the limit load needs to be known. However for dynamic problems the ultimate displacement is necessary as the maximum strain energy of the member needs to be derived exactly [1, 4, 9].

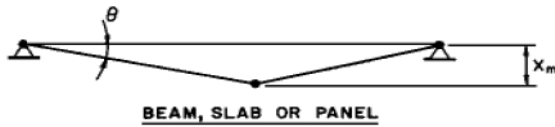


Figure 5: Hinge Definition according to [9]

This issue has been solved by the definition of limits for the support rotation. The UFC 3-340-02 [9] recommends a value of 2° for regular design purposes, where crushing of the concrete is unfeasible.

The definition of a maximum rotation has a direct impact on the dynamic response results as the rotation defines the maximum displacement and hence also the strain energy *S.E.* of the system.

$$S.E. = \int r(u) du \quad (5)$$

As the strain energy defines the dynamic resistance in the impulsive and dynamic domain of response it is necessary to derive the maximum rotation accurately and therefore questionable if a general definition is appropriate.

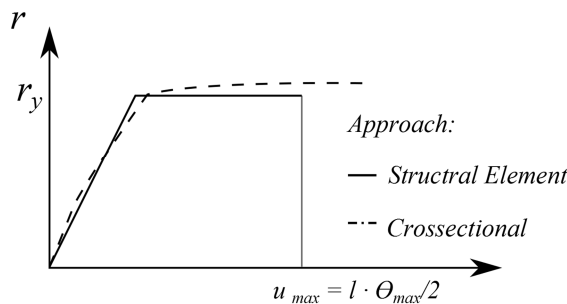


Figure 6: Schematic Load-Displacement function for structural element and crosssectional approach.

Therefore reinforced-concrete elements can be designed using elasto-plastic limit analysis. With the structural element approach being a simplification of the crosssectional approach (see figure 7) as curvature and plastic hinge rotation are directly related. The general influences on the rotation capabilities are shown within the following.

HINGE ROTATION

The rotation is defined by the integration of the curvature along a given length of the member. For elastic θ_{el} and plastic rotation θ_{pl} different definitions can be found i.e. by Dilger [11], Bachman [13], and the CEB [15]. These definitions may vary in their description of the integration length of the plastic hinge and the definition of elastic and plastic curvature (figure 7).

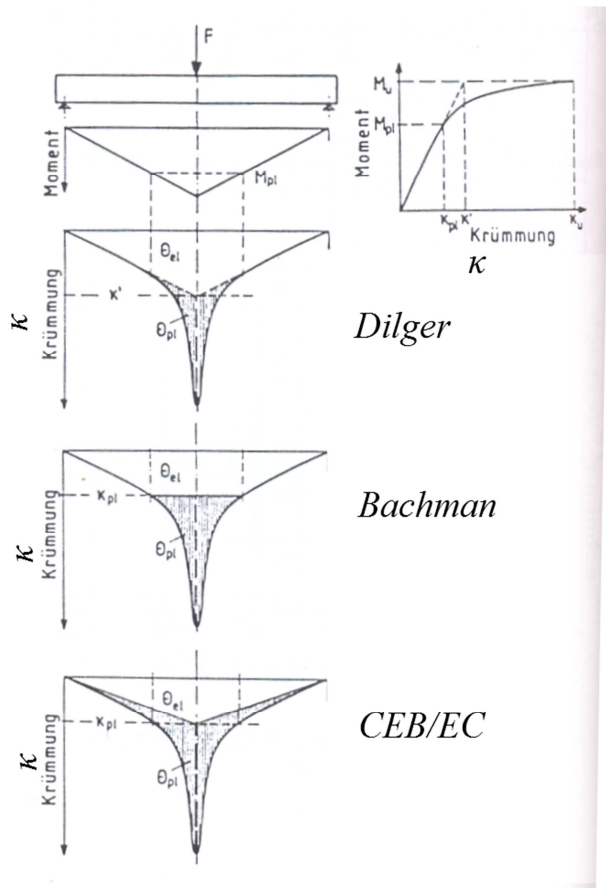


Figure 7: Schematic definition of the elastic rotation and plastic rotation from Langer [14]

But independent from the definition, the maximum plastic rotation is defined by two main characteristics [15]:

The *Shear Slenderness* defines the size of the plastic region. Given by the fraction of the distance between maximum and zero bending moment ($\approx M/V$), and the effective height of the reinforcement within the crosssection *d*.

$$\lambda = M/V \cdot d \quad (5)$$

The *Normed Height of Compression Zone* (ξ) and the *ductility of concrete and steel* define the ductility on the cross sectional level. Either by crushing of the concrete (ε_{cu}) or rupture of the reinforcement (ε_{su}) related to κ_u by equation 6.

$$\kappa_u = \varepsilon_{cu}(\xi) \cdot d \quad \text{concrete failure}$$

$$\kappa_u = \varepsilon_{su}(1-\xi) \cdot d \quad \text{steel failure} \quad (6)$$

Therefore the maximum plastic rotation is limited to reinforcement or concrete failure as indicated by figure 9 according to the EC [15].

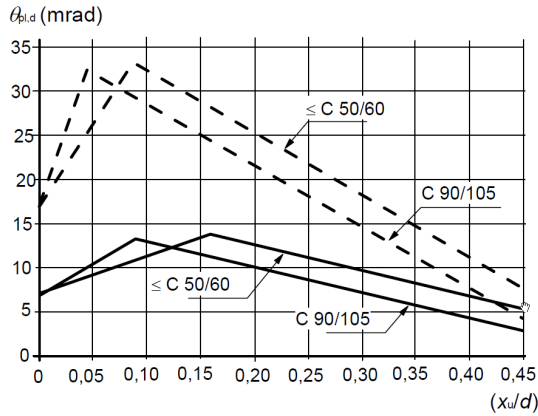


Figure 8: Plastic Rotation limits according to EC for $\lambda = 1.0$ and reinforcement of Class B (straight line) and Class C (dotted line) [15].

As stated by figure 9 a general definition of a maximum rotation is not possible, as the maximum value depends on the height of the compression zone which indicates the failure mechanism (concrete or steel), the ductility of the steel and the size of the plastic region. Therefore the total rotation is directly affected by the reinforcement ratio, axial loading, boundaries and the loading type. This is in contrast to the recommendation stated within the UFC [9], which defines one general rotation limit.

3 COMPARISON OF SDOF-METHODS

Based on four shocktube tests on reinforced

concrete plates the applicability of the FEM and SDOF method for the description of dynamic loads has been examined. The shock tube test were carried out at the Fraunhofer EMI (figure 13 and table 1).

The maximum strain rate observed using hydrocode simulations were in the range of 10^{-3} [1/s]. Therefore the maximum increase of the tension strength for the concrete is around 10% according to [13], therefore the SDOF method can be used as the effect of strain rates are negligible.

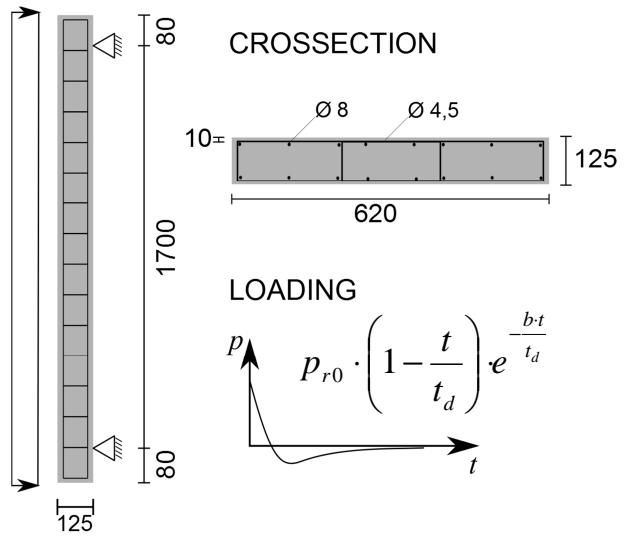


Figure 9: Loading and Dimension of RC-Elements.

Table 1: Material Properties for Concrete and Reinforcement and Loading for Tests G 957-959

Material Properties			
Concrete – C 50 [23]			
E_{cm}	youngs modulus	38500	[N/mm ²]
f_{cm}	compression strength	58	[N/mm ²]
f_{ct}	tension strength ¹	4,1	[N/mm ²]
Steel			
E_{sm}	youngs modulus	210000	[N/mm ²]
f_y	yield stress	500	[N/mm ²]
f_u	ultimate stress	550	[N/mm ²]
¹ calculated according to CEB[23]			
Loading			
	P_{r0} [kN/m ²]	b	t_d [ms]
G956	53	0.62	21
G957	105	0.93	29
G958	152	1.11	37
G959	202	1.25	42

The SDOF analysis states crushing of concrete as a failure mechanism as indicated by the shape and relatively low ductility of the load displacement curve (figure 13). Both displacement curves have been calculated using the cross-sectional approach and the structural element approach according to [9] with a maximum support rotation of 2° .

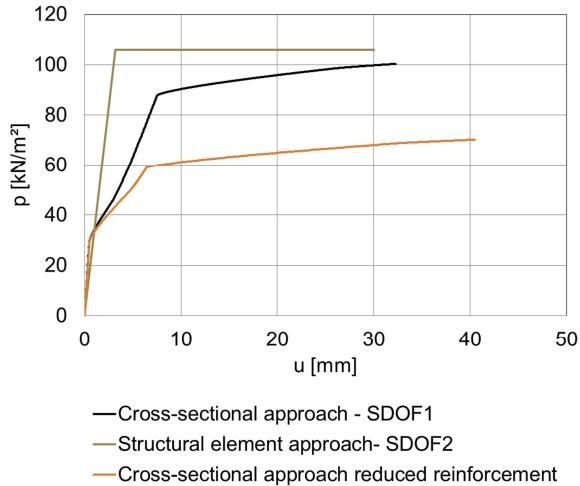


Figure 10: Load displacement-curves for cross-sectional approach with reduced and full reinforcement and for SDOF-2 according to [9].

Hereby the following differences can be stated:

The structural element approach of the UFC-3-340 overestimates the maximum moment resistances, as a rectangular stress block for the concrete is hereby chosen for the evaluation of the maximum resistance, which overestimates the internal cantilever and hence the maximum moment and resistance. Also the average stiffness is overestimated. The maximum displacement between of the element used in the experiment and the cross-sectional approach is comparable. This is due to the “right” choice of the reinforcement ratio. As shown in figure 13 for a reduction of the reinforcement of 33% the displacement increases for the cross-sectional approach which is in contrast to the structural-element approach of the UFC-3-340.

The dynamic analysis using the cross-sectional approach (SDOF 1) showed a good agreement for G957 and G958 with the

experimental data (figure 13) and was able to describe the progression of displacement until the first excitation after 15ms and 20ms nicely. Only for low dynamic loads (G956) the numerical and experimental results differ, which may be reasoned by a deviation of the tensile strength to the material properties stated in table 1 according to [23] or due to a small of the support boundary.

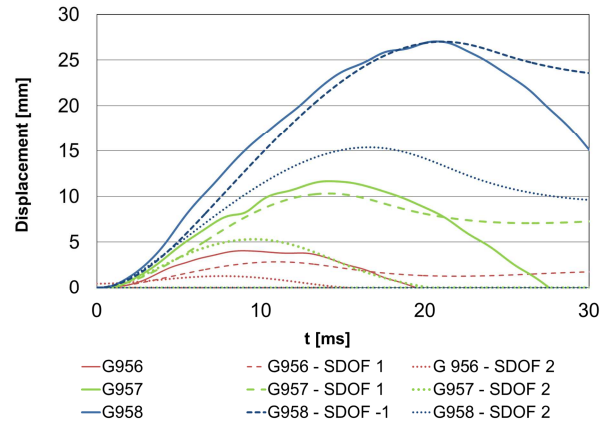


Figure 11: Measured displacement at mid-span and numerical results of SDOF 1 and SDOF 2 for experiment G956, G 957 and G958.

The structural element (SDOF 2) approach showed a larger deviation from the experimental results compared to the cross-sectional approach (table 2), even though both approaches need the same parameters as an input (concrete strength, reinforcement strength, dimensions).

Table 2: Maximum displacements of test series and the deviation of the numerical analysis.

	u_{Exp} [mm]	deviation	
		SDOF -1	SODF-2
G956	4,0	-40 %	-75 %
G957	11,7	-13 %	-55 %
G958	27,0	~0%	-41 %
G 959		failure	

The deviation can be related to the load-displacement curve shown in figure 13. The structural-element approach overestimates the resistance and average stiffness until yielding of the steel occurs, which lead to lower displacements within the numerical

calculations for the same strain energy.

For experiment G959 failure was given within the experiment and also predicted by both numerical methods.

Compromising it may be stated, that the cross-sectional approach was able to describe the experimental results more accurate than the structural element approach, even though both approaches use the same input parameter. It may be possible to identify better bilinear approximation (structural-element-approach) for the load displacement curve. However hereto other techniques, such as the FEM or cross-sectional approach need to be used as a reference for the load displacement curve in advance, this would question the structural element approach as other more elaborate and accurate approaches need to be used anyway. Even so the structural-element approach can be used as an approximation of a load-displacement curve to determine general effects of preload as will be shown in chapter 4.

4 EFFECTS OF PRELOAD

Many experimental tests of members subjected to impact or blast loads have been carried out and the behaviour of reinforced concrete may be described from the dynamic to the impulsive domain. However aspects of preloading are generally neglected within the experimental setup due to the complexity of the experimental configuration or even within the design of members. Numerical analyses of Krauthammer [2], Stolz and Riedel [1] indicate the effects of axial preloads on the structural behaviour of reinforced concrete members. The influence of transverse preloads on structural members and their dynamic response can be described by their influence to the quasi-static p_{min} and impulsive limits i_{min} of the dynamic response of members. These limits are defined by equilibrium of internal and external energy [7, 9] according to (6) and (7).

$$\int r(u)du \equiv \frac{mV^2}{2} = \frac{i_{min}^2}{m \cdot 2} \quad (6)$$

$$\int r(u)du \equiv p_{min} \cdot u \quad (7)$$

The response of reinforced concrete members can be approximated with a elasto-plastic load displacement function, bearing in mind the issues discussed in 2 and 3. This function can further be generalized to analyse the effects of preload for arbitrary members with different ductilities and degrees of preload. The general parameters thereto are the resistance r , the elastic displacement u_{el} , maximum displacement u_{ul} , the ductility β defined as the ratio of elastic to plastic deformations, the preload q_0 , the displacement at preload u_0 and the degree of preload α (figure 12).

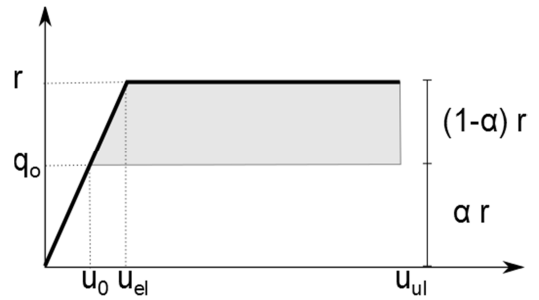


Figure 12: General bilinear load displacement function.

With the general load displacement curve boundaries for the impulsive and quasi static response can be derived for a given degree of preload. Hereby it is assumed that the preload is not participating as an additional mass to the excitation of the system, hence m and α are independent. According to (6) and (7) it follows:

$$i_{min} = \sqrt{2mu_{el}r \left(\frac{(1-\alpha)^2}{2} + \beta \cdot (1-\alpha) \right)} \quad (8)$$

$$p_{min} = \frac{r \cdot \left(\frac{(1-\alpha)^2}{2} + \beta \cdot (1-\alpha) \right)}{(1 + \beta - \alpha)} \quad (9)$$

The values for linear systems are satisfied by (8) and (9) for $\beta=0$ and $\alpha=0$ the impulsive limit equals $(m u_{el} r)^{0,5}$ and the quasi-static limit equals $r/2$, which is in accordance with [7, 9]. From Equation (8) and (9) the error caused by neglecting pre load as given dead loads on the quasi-static and impulsive response of structures can be determined (10) and (11).

$$\begin{aligned} \text{error} - p_{\min} &= 1 - \frac{p_{\min}}{p_{\min}(\alpha=0)} \\ &= 1 - \frac{\frac{(1-\alpha)^2}{1+2\cdot\beta} + \frac{1-\alpha}{1/(2\beta)+1}}{1 - \frac{\alpha}{1+\beta}} \end{aligned} \quad (10)$$

$$\begin{aligned} \text{error} - i_{\min} &= 1 - \frac{i_{\min}}{i_{\min}(\alpha=0)} \\ &= 1 - \sqrt{\frac{\frac{(1-\alpha)^2}{2} + \beta(1-\alpha)}{1/2 + \beta}} \end{aligned} \quad (11)$$

Figure 13 represents the error caused by neglecting preloads. The arising error is between 15 % and 55% for typical degrees of preload from 25 % to 60% of the maximum resistance in bending.

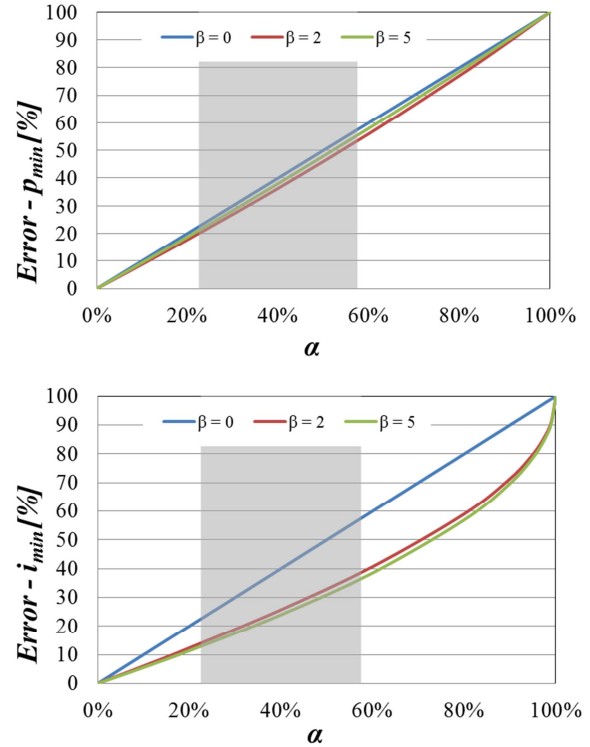


Figure 13: Error by neglecting preload for p_{\min} and i_{\min} and different ductilities β (shaded area represents typical degrees of preload due to dead loads).

For the member analysed in 5 the minimum impulse and minimum quasi-static pressure can be determined according to equation (8), (9) and figure 13 ($m=0,259$ t/m²; $\beta=3,3$; $u_{el}=7,5$ mm; $r = 97,5$ kN/m²) to $i_{\min} = 1,2$ kN/m²s and $p_{\min}=86$ kN/m². Equations 10 and 11 can be used for the estimation of the reduction for the quasi-static and impulsive limits for a given pre load. Assuming reasonable degrees of preload of 20 and 40% the reduction in p_{\min} and in i_{\min} is equal to 18% and 37% and 12 % and 25% respectively.

These values are verified by the pressure impulse diagrams of the reinforced concrete members analysed in 3 with the load displacement function according to figure 14 (cross-sectional approach) and different degrees of preload. Hereby a triangular loading shape has been used and a search algorithm according to [27].

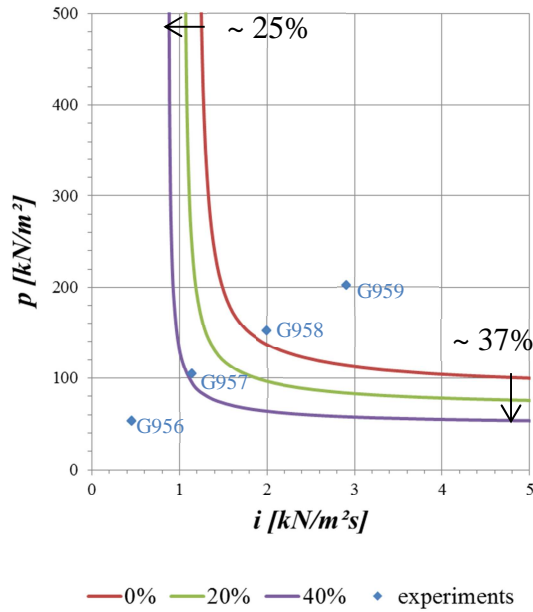


Figure 14: Pressure-Impulse-Diagrams for triangular loading including no and preload in degrees of 20% (green) and 40% (red).

In contrast to the numerical and experimental results failure is indicated by the PI-Curves for experiment G957 which is reasoned by the shape of the load distribution. This shape is different for the PI-diagrams and the experimental configuration which affects the PI curves and therefore indicates damage for experiment G957, this aspect has already been represented by Krauthammer [17].

The PI-curves with different degrees of preload confirm the formulas for the reduction of the quasi-static and impulsive limits and show a significant reduction in the dynamic resistance. This indicates the relevance for the consideration of preloads for the description of structural behaviour and dynamic resistance.

5 HYDROCODE SIMMULATIONS

As beforehand shown the SDOF-approach enables the description of reinforced concrete members resisting in a bending mode subjected to blast-load. However for arbitrary problems a general methodology for the description of reinforced concrete is necessary as the behaviour may not be dominated by bending effects or an equivalent SDOF may

not be easily determined.

A general methodology hereto is given by the Finite Element Method (FEM), whereas different approaches are feasible, i.e. classical implicit FEM, particle methods or hydrocode formulation. As a result of its explicit formulation the hydrocode formulation includes the equation of state together with a constitutive law for the material description and the conservation laws of mass, momentum and energy [18]. Therefore wave and shockwave propagation problems can be described with reasonable computational effort. This allows for the description of concrete and reinforced concrete for structural dynamic and high speed dynamic loads [1, 4, 19, 20].

Numerical analysis of the experiments stated in 3 using the hydrocode are in a good agreement with the experiments, see figure 14. Hereto the concrete has been modelled using the RHT Model [16] and Lagrange Elements and the reinforcement was modelled using discrete beam elements and the description according to Johnson-Cook [22].

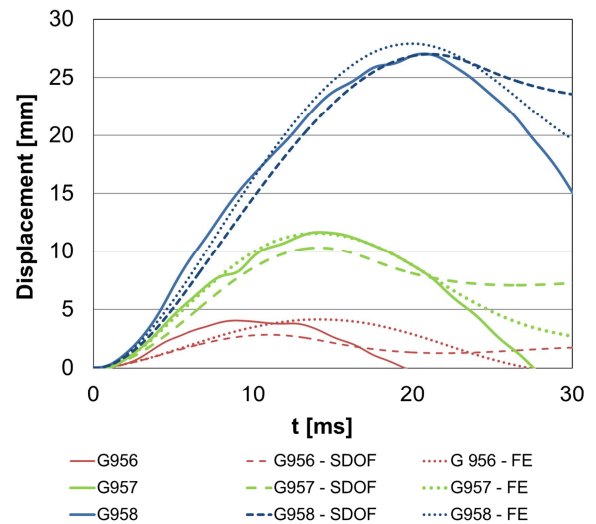


Figure 15: Measured displacement at mid-span and numerical results of SDOF-1 and FE for experiment G956, G 957 and G958.

For a first indication preload has been included in the hydrocode as well as the SDOF method using the dynamic load of G957 and a transverse preload (q_0) of 15 kN/m². As

presented in figure 16 an increase of displacement is predicted by both methods, due to the presence of preload at the onset of dynamic loads.

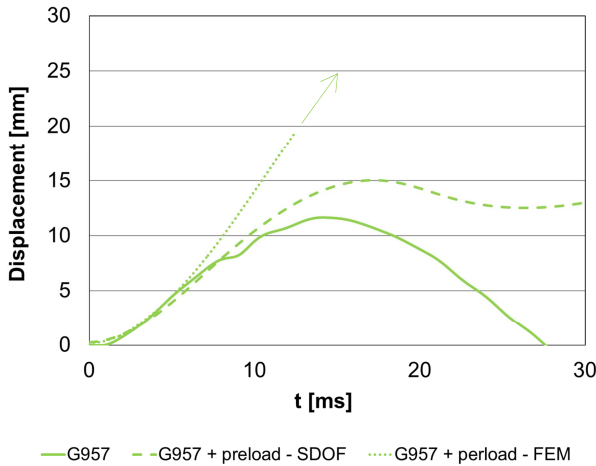


Figure 16: Effects of preload on numerical results using FEM and SDOF analysis and experimental results of G957 without preload.

As both methods predict more deformations, the damage of the member also increases as shown in figure 17 for the backside of the member in the hydrocode simulation.

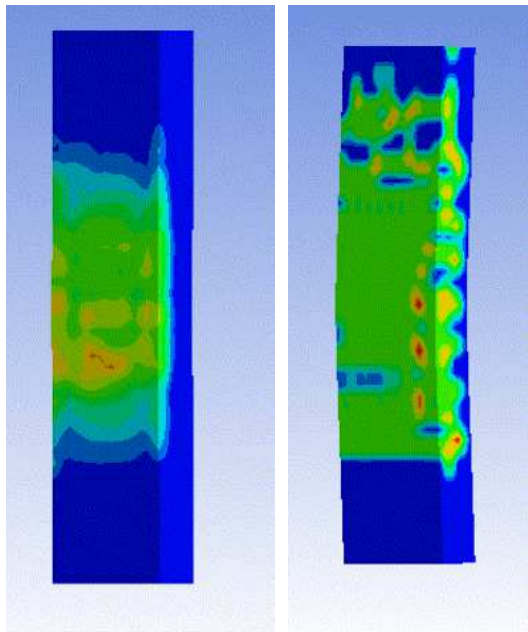


Figure 17: Damage on the backside of the plate without preload (left) and with preload (right)

As shown in figure 16 the hydrocode simulation predicts larger deformations in contrast to the SDOF method, hereto further investigations for the distinction of both methods under the aspect of preload are necessary and will be carried out in the future.

7 CONCLUSIONS

Different approaches for the analysis of reinforced concrete elements under different loading rates have been represented. The applicability of the cross-sectional SDOF for the description of the dynamic behaviour of reinforced concrete elements against blast loads has been shown on shock-tube test. For an indication of the effects of transverse preload formulas for the influence of preload on the boundaries of dynamic behaviour, the impulsive and quasi-static limits, for elastoplastic resistance functions have been derived. These formulas have been verified using generated PI-diagrams and indicate the necessity for the consideration of preloads. As a first test simulations using hydrocodes and SDOF analysis have been performed, which also show a large influence of preload on the structural behaviour.

Future experiments on axial and transversal preloaded reinforced concrete elements under shock loads will be carried out at the Fraunhofer EMI, which will help to validate and extend the present methodologies for the description of reinforced concrete members under different loading rates and preloaded conditions.

REFERENCES

- [1] Riedel, Stolz, Roller, Nöldgen, Laubach, Pattberg, 2011. *Impact Resistant Superstructure for Power Plants Part I: Box Girders and Concrete Qualities*, Proc. 21st Structural Mechanics in Reactor Technology.
- [2] Krauthammer, Astarioglu, 2010. *Short Reinforced Concrete Columns under Combined Axial and Blast-induced Transverse Loads*, Proc. 3rd International Conference on Design and Analysis of

- Protective Structures. 198.
- [3] UFC-3-340-02, 2008. *Structures to Resist the Effects of Accidental Explosions*, U.S. Army Corps Of Engineers.
- [4] Chopra, 1995. *Dynamic of Structures*, 1st Edition, Prentice Hall..
- [5] Lestuzzi, Bachmann, 2007. *Displacement ductility and energy assessment from shaking table tests on RC structural walls*, Eng. Structures **29**:1708-1721.
- [6] Biggs, 1964. *Introduction to Structural Dynamics*, McGraw-Hill.
- [7] Krauthammer, 2008. *Modern Protective Structures*, Taylor & Francis.
- [8] Blasko, Krauthammer, Astarlioglu , 2007. *Pressure–impulse diagrams for structural elements subjected to dynamic loads. Technical report PTC-TR-002-2007*, Pennsylvania State University.
- [9] Cormie, Mays, Smith, 2009. *Blast Effects on Buildings*, 2nd edition, Thomas thelford.
- [10] Ritz, 1906. *Über eine neue Methode zur Lösung gewisser Variationsprobleme der mathematischen Physik*, Journal für die Reine und Angewandte Mathematik **135**: 1–61.
- [11] Dilger, 1966. *Veränderlichkeit der Bieg- und Schubsteifigkeit von Stahlbetontragwerken und deren Einfluß auf Schnittkraftverteilung und Traglast bei statisch unbestimmter Lagerung*, Deutscher Ausschuss für Stahlbeton, **179**.
- [12] Leonhardt F., 1978. *Vorlesungen Über Massivbau: Vierter Teil 4: Nachweis der Gebrauchsfähigkeit Rissebeschränkung, Formänderungen, Momentenumlagerung und Bruchlinientheorie im Stahlbetonbau*, 2nd edition, Springer.
- [13] CEB-FIP, 1993. *Model Code 90*, Thomas Telford, London.
- [14] Langer, 1997. *Verdrehfähigkeit plastifizierter Tragwerksbereiche im Stahlbetonbau*, Deutscher Ausschuss für Stahlbeton, **484**:127-
- [15] Bachmann, 1967. *Versuche über das plastische Verhalten von zweifeldrigen Stahlbetonbalken*, Dissertation, ETH-Zürich.
- [16] EC 1992-1, 2004, *Design of concrete structures*, CEN
- [17] Krauthammer, Astarlioglu, Blasko, 2008. *Pressure–impulse diagrams for the behavior assessment of structural components*, International Journal of Impact Engineering **35**: 771–783.
- [18] Hiermaier, 2003. *Numerik und Werkstoffdynamik der Crash- und Impaktvorgänge*, é-Forschungsberichte aus der Kurzzeitdynamik, Fraunhofer-Verlag.
- [19] Riedel, 2009. *Numerical assessment for impact strength measurements in concrete materials*, Int. Journal of Impact Engineering **36**: 283-393.
- [20] Nöldgen, 2011. *Modelling of ultra-high performance concrete under impact loading*, é-Forschungsberichte aus der Kurzzeitdynamik, Fraunhofer-Verlag.
- [21] CEB-FIP, 2012. *Model Code 2010*, bulletin 65.
- [22] Century Dynamics, 2002. *Autodyn - Theory Manual*.